Amorphization in Gd–Co alloys and multilayers

2002 J. Phys.: Condens. Matter 14 8913

(http://iopscience.iop.org/0953-8984/14/39/301)

INSTITUTE OF PHYSICS PUBLISHING JOURNAL OF PHYSICS: CONDENSED MATTER

J. Phys.: Condens. Matter **14** (2002) 8913–8924 PII: S0953-8984(02)37389-2

Amorphization in Gd–Co alloys and multilayers

J A Alonso[1], R Hojvat de Tendler[2], D A Barbiric[3] and J M Riveiro[4]

[1] Departamento de Física Teórica, Universidad de Valladolid, 47011 Valladolid, Spain
[2] Instituto de Estudios Nucleares, Centro Atómico Ezeiza, CNEA, 1429 Buenos Aires, Argentina
[3] Departamento de Química Inorgánica, Analítica y Química Física, Universidad de Buenos Aires, 1428 Buenos Aires, Argentina
[4] Departamento de Física Aplicada, Universidad de Castilla-La Mancha, 13071 Ciudad Real, Spain

Received 15 May 2002
Published 19 September 2002
Online at stacks.iop.org/JPhysCM/14/8913

Abstract

A semiempirical model is used to analyse the results of published experiments reporting on the solid-state amorphization reactions in bilayers and multilayers formed by Gd and Co. The role of the interfacial effects in raising the free energy of the initial arrangement in a multilayered configuration, and in promoting the amorphization reaction, is studied in detail. The model explains the observation of amorphous alloys over a broad composition range in the bilayer experiments. The preferred composition obtained in the multilayer experiments is discussed critically and the model prediction of a preferred composition $Gd_{0.46}Co_{0.54}$ is in good agreement with the compositions observed in recent experiments.

1. Introduction

Rare-earth–cobalt alloys are materials of interest for magneto-optics applications [1]. The antiparallel coupling between a ferromagnetic rare earth, such as Gd, and a ferromagnetic transition metal, such as Fe or Co, results in a variety of spin configurations in thin multilayers [2]. For this reason, bilayers [3] and multilayers [4, 5] have been prepared in the Gd–Co system and interfacial reactions have been reported to occur. X-ray diffraction and transmission electron microscopy measurements performed by Hufnagel and co-workers [3] indicate a fast amorphization reaction when Co is deposited on thin Gd films. Riveiro and co-workers [4, 5] prepared Gd/Co bilayers and multilayers by sputter deposition on glass substrates at room temperature. In the experiments on single bilayer films of overall composition $Gd_{1-x}Co_x$ they observed [4] the formation of totally amorphous alloys for compositions $x > 0.25$ up to at least $x = 0.60$, in agreement with previous reports [6]. In the case of multilayers, the samples formed in this way had 20 bilayers and their structure and composition were analysed before and after reaction. Low-angle reflectivity and conventional x-ray diffraction were used for structural and thickness determination, and energy-dispersive x-ray microanalysis provided the bulk composition. Auger electron spectroscopy combined with controlled ion etching was used to measure composition–depth profiles. The analysis indicates

that a strong amorphization reaction occurs at the interfaces between Co and Gd layers. The composition as a function of depth can only be explained by a model of asymmetric diffusion through the interfaces, the diffusion of Co into Gd being predominant.

In more detail, in a set of experiments on multilayers [4] in which the thickness of the individual Gd layers was set at 50 Å while the thickness of the Co layers varied from 14 to 210 Å, the observation was made that a part of each Co layer remains unreacted when the original thickness of the Co layers is greater than 100 Å. In another set of experiments [4, 5] with various thicknesses of the Gd and the Co layers, an attempt was made to determine the composition–depth profile of the amorphous alloy using a method of analysis that combines Auger spectroscopy with controlled ion etching. The measurements showed that the interfacial reaction transforms the original Gd layers into an amorphous alloy, bound by thinner Co layers corresponding to the unreacted part of the initial Co layers. The estimate of the preferred composition of the amorphous $Gd_{1-x}Co_x$ alloy given in those papers [4, 5] was $x = 0.29$–0.35, which is near the composition $Gd_{0.63}Co_{0.37}$ of the eutectic point of the alloy [7].

However, low-angle reflectivity scans performed recently on the old samples of [4] and [5] showed that the homogeneity of their compositions was not good and those were actually modulated alloys. The reason is that the method used to prepare the initial multilayer arrangements in [4] and [5] produced multilayers with rough interfaces instead of sharp ones, and this occurred because the sputtering apparatus used in those works had only one radio-frequency (RF) generator available, which meant that it had to be switched on and off for every layer, from Co cathode to Gd cathode. This switching results in a slower and more uncontrolled deposition process. Consequently, additional experiments have been recently performed [8, 9] with the intention of determining more accurately the preferred amorphous composition. A significant improvement introduced in the experimental procedure consists in the use of a two-RF-generator set, so the two plasmas are kept on during the full growth time. This change resulted in sharper interfaces in the initial multilayer arrangement and in a better homogeneity of the alloys formed by the solid-state reaction. Another crucial difference is that the initial multilayers prepared in the new experiments are formed by alternated a-($Gd_{1-x}Co_x$) and Co layers, where a-($Gd_{1-x}Co_x$) represents an amorphous alloy layer with composition $Gd_{1-x}Co_x$ and the Co layers are evidently crystalline. Three values of x were chosen: the eutectic composition $x = 0.37$; a composition $x = 0.60$, rich in Co; and a composition $x = 0$, in which case the multilayers are simply *pure* crystalline Gd/Co multilayers. The Co diffusivity into the amorphous layers was monitored by electrical resistivity measurements for temperatures between 8 and 300 K. The advantage of these novel configurations is that the experiments on the a-($Gd_{0.63}Co_{0.37}$)/Co multilayers provide a stringent test of the preferred amorphous composition. If the preferred composition is the eutectic one, further reaction to produce additional Co enrichment of the amorphous alloy is not expected. In contrast, the result of the experiment [8, 9] is that reaction occurs and the eutectic layers become substantially enriched in Co. This enrichment is revealed by an increase of the room temperature resistivity. Furthermore, measurements for the three series of multilayers lead to the same conclusion: Co enrichment of the amorphous alloy proceeds up to a limiting composition not far from $Gd_{0.40}Co_{0.60}$. Once the limiting composition is reached, the rapid fall of the resistivity indicates that the interdiffusion stops.

These results have been confirmed by independent experiments [10] for a-($Gd_{1-x}Co_x$)/Co multilayers with $x = 0$, 0.37, 0.53 and 0.60. In those experiments the amount of Co diffused into the amorphous alloy was determined by transverse magneto-optic Kerr effect (T-MOKE) measurements. Appreciable diffusivity was observed for the case with $x = 0.37$, with a mean composition of the enriched alloy equal to $Gd_{0.46}Co_{0.54}$. On the other hand, the diffusivity of Co was clearly impeded for the cases of $x = 0.53$ and 0.60.

In this paper we perform a theoretical analysis of the amorphization in the Gd–Co system using a semiempirical theory [11–14] and give, first of all, support for the broad amorphization range found in the simple bilayer experiments. On the other hand, the calculations give support to the preferred amorphous composition near $Gd_{0.40}Co_{0.60}$ obtained in the recent multilayer experiments [8–10].

Co–Gd is just a member of a broad class of alloys in which fast diffusion of one of the elements into the other allows formation of amorphous alloys by the techniques of solid-state reaction of multilayers [15] and ball milling [16]. The amount of information existing on Co–Gd [3–5, 8–10] explains its selection as a representative example of this interesting class of materials.

2. Phenomenological description of the amorphization range

In a mixture of two metals, there is a thermodynamic driving force for amorphization when the free energy of the amorphous alloy is lower than the concentration average of the free energies of the component crystalline metals. This is the case in figure 1. The pure crystalline metals set the zero of energies and the continuous curve labelled a represents the Gibbs free energy of formation ΔG_a of the amorphous alloy $Gd_{1-x}Co_x$ at $T = 300$ K. Curve a is below the horizontal zero-line, except very close to $x = 0$ and 1. ΔG_a has been calculated using a semiempirical theory [11–14]. More precisely,

$$\Delta G_a(x) = (1-x)\,\Delta G^{\mathrm{c-l}}(\mathrm{Gd}) + x\,\Delta G^{\mathrm{c-l}}(\mathrm{Co}) - T\,\Delta S_a(x) + \Delta H_a(x). \quad (1)$$

To understand this equation, one can imagine a *model* in which the amorphous phase is produced in two steps: first melting the two crystalline metals at a temperature T below their normal melting temperatures and then mixing the two undercooled liquids. $\Delta G^{\mathrm{c-l}}(\mathrm{Gd})$ and $\Delta G^{\mathrm{c-l}}(\mathrm{Co})$ are the free energy changes associated with the crystal–liquid (c–l) transition in the first step, that is the free energy difference between the undercooled liquid (l) and the crystalline (c) phases of the pure metals. This contribution is responsible for the positive values of ΔG_a near $x = 0$ and 1. The mixing is described by the last two terms of equation (1). $\Delta S_a(x)$ is the entropy of mixing of the two liquid metals and $\Delta H_a(x)$ is the enthalpy of mixing. A good approximation for $\Delta G^{\mathrm{c-l}}$ for pure metals is [17]

$$\Delta G^{\mathrm{c-l}} = \alpha(T_m - T) \quad (2)$$

where T_m is the melting temperature (see table 1), and α is an empirical best-fit parameter with a value 3.5 J mol^{-1} K^{-1}, the same for all metals. For the entropy of mixing ΔS_a, we have taken the Flory's expression [18]; this is a simple approximation taking into account the size differences between the Co and Gd atoms. Finally, ΔH_a is the enthalpy of mixing, given by Miedema's model [11] in the form

$$\Delta H_a = x(V_{\mathrm{Co}}(\mathrm{alloy}))^{2/3} f(x)\,\Delta H^{amp} \quad (3)$$

where ΔH^{amp} is an amplitude reflecting the magnitude of the chemical interaction. This amplitude depends on the difference of the average electron densities at the boundary of the atomic cells of the two pure metals, $n_{\mathrm{Co}} - n_{\mathrm{Gd}}$, and on the difference of the electronic chemical potentials (or electronegativities), $\Phi_{\mathrm{Co}} - \Phi_{\mathrm{Gd}}$, and its precise expression can be seen in [11], which also gives the values of the relevant parameters Φ and n. $V_{\mathrm{Co}}(\mathrm{alloy})$ is the effective molar volume of Co in the alloy (see also [11]) and $f(x)$ is a function of the concentration that accounts for the degree of chemical short-range order in the alloy. The expression

$$f(x) = x^s_{\mathrm{Gd}}[1 + \eta(x^s_{\mathrm{Co}}x^s_{\mathrm{Gd}})^2] \quad (4)$$

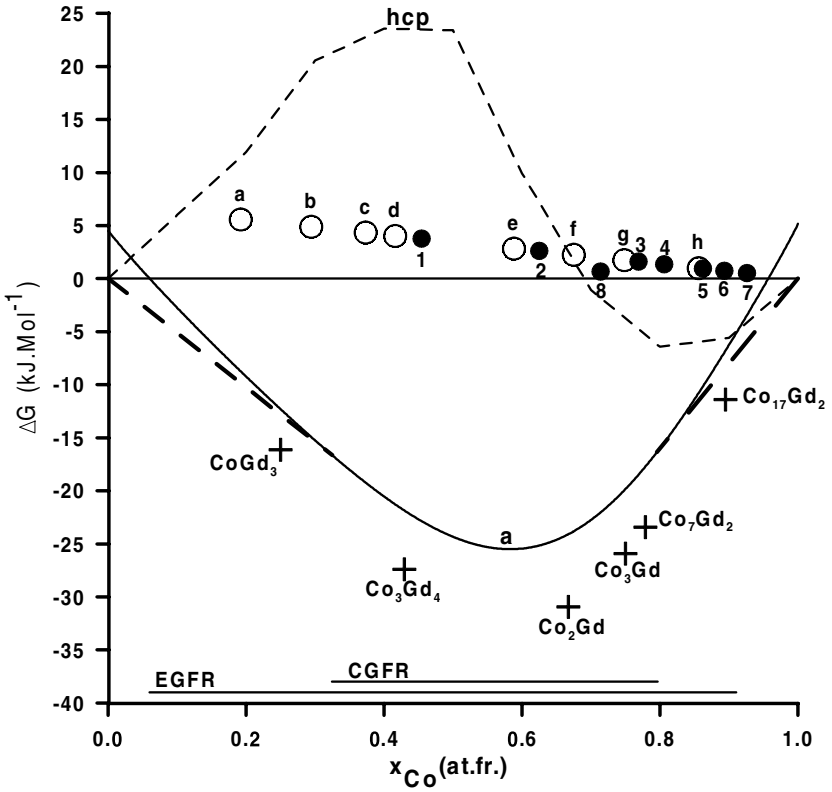

Figure 1. Calculated room temperature Gibbs free energies of the amorphous (a) and solid-solution (hcp) phases in the $Gd_{1-x}Co_x$ alloy, measured with respect to the pure solid metals. Predicted regions of complete glass formation or extended glass formation are indicated at the bottom (see the text). The CGFR is determined by the common tangent (long-dashed) lines. Calculated free energies of the intermetallic compounds with the compositions indicated are given by the crosses. Filled circles 1–8 represent the free energy of the initial unreacted configuration in the case of the Co/Gd multilayers of [4], and open circles a–h correspond to the pure Co/Gd multilayers of [8].

Table 1. The main parameters used in some of the equations of this work.

Metal	Melting temperature T_m (K)	Molar volume of pure metal V (cm^3)	Surface energy γ (mJ m^{-2})	Enthalpy of solution ΔH^0 (kJ mol^{-1})
Co	1768	6.689	2550	−67 (Co in Gd)
Gd	1586	19.886	1110	−112 (Gd in Co)
References	[7]	[11]	[11]	This work

controls the degree of chemical short-range order through the parameter η ($\eta = 0$ for random solid solutions and $\eta = 8$ for fully ordered alloys; in the case of amorphous alloys the intermediate value $\eta = 5$ is recommended [19]). The superscript s means that the concentrations x^s_{Co} and x^s_{Gd} appearing in equation (4) are atomic cell surface area concentrations. The different contributions to ΔG_a are plotted in figure 2, and the dominant role of the enthalpy of mixing ΔH_a is evident.

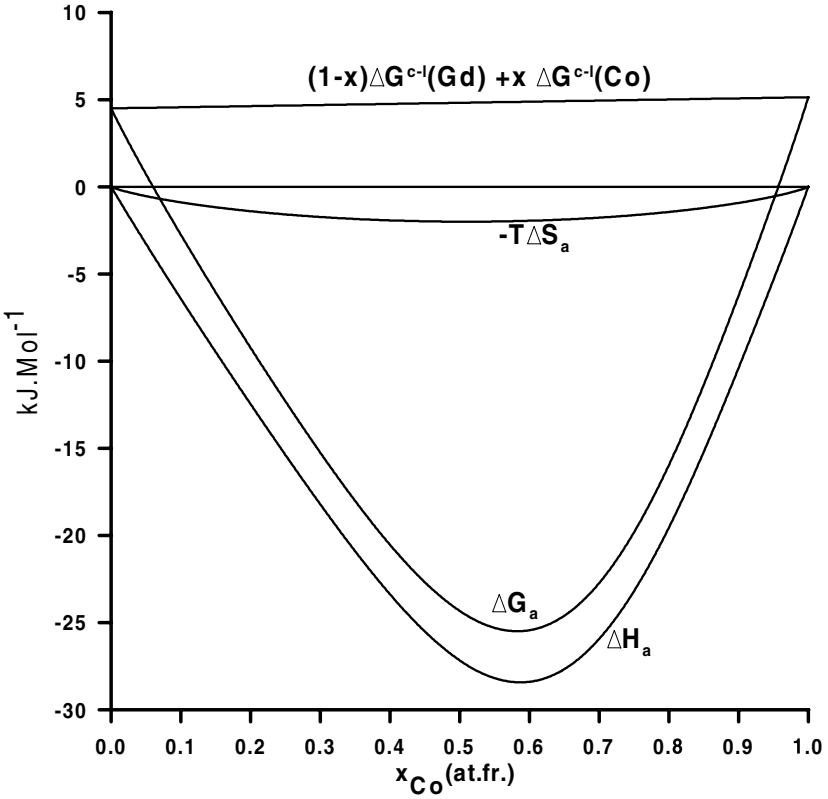

Figure 2. Different contributions to the free energy of formation ΔG_a of the amorphous $Gd_{1-x}Co_x$ alloy (see equation (1) of the text) as a function of the Co concentration (atomic fraction).

As indicated above, the $\Delta G_a(x)$ curve in figure 1 has negative values in most of the concentration range. The curve is weakly asymmetric, with a minimum for $x = 0.58$. Amorphous alloys could then form provided that the formation of ordered stoichiometric crystalline compounds is kinetically avoided. This is the case in the usual fast-quenching techniques. For the technique of solid-state reaction of multilayers discussed here, the main factor in avoiding the formation of the ordered compounds is the low diffusivity of Gd at the working temperature, which prevents the formation of compound nuclei. However, formation of crystalline dilute solid solutions is more difficult to prevent, and these compete with the formation of amorphous alloys for concentrations near $x = 0$ and 1. In addition, one can appreciate in figure 1 that it would be hard to form amorphous alloys near those terminal regions because $\Delta G_a(x)$ is positive there. To give the full picture we have plotted in figure 1 the free energy of formation of random (not short-range-ordered) substitutional hcp solid solutions, $\Delta G_{ss}(x)$, given as a short-dashed curve, labelled hcp. This was obtained by adding several contributions:

$$\Delta G_{ss} = \Delta H_{chem} + \Delta H_e + \Delta H_{str} - T\,\Delta S_{ss} \tag{5}$$

where the first three terms are enthalpy terms that we now discuss and the last one is an entropy term. The term ΔH_{chem} is a chemical interaction, essentially identical to ΔH_a of equation (3), with the only difference being a possibly different value for η in equation (4). We have chosen $\eta = 0$ for the solid solution (if $\eta = 0$ is also taken for the amorphous alloy, a slightly less

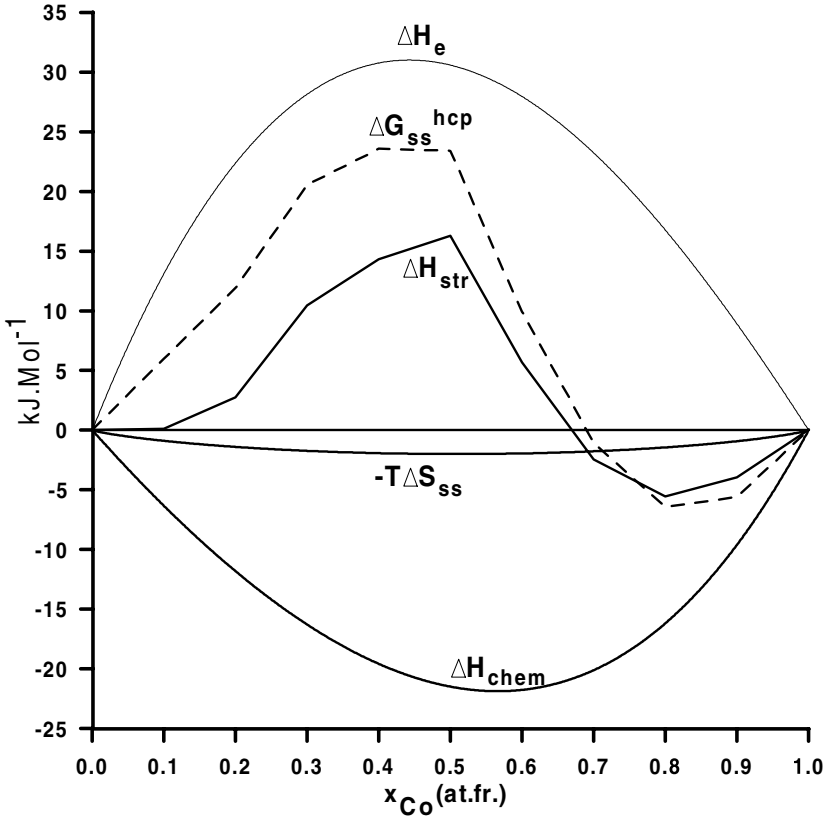

Figure 3. Different contributions to the free energy of formation ΔG_{ss} of the hcp $Gd_{1-x}Co_x$ solid solution (see equation (5) of the text) as a function of the Co concentration (atomic fraction).

negative ΔG_a curve would be obtained; however, the whole picture of figure 1 would be the same). ΔH_e is an elastic energy term accounting for atomic size mismatch, typical of solid solutions. Its practical expression in terms of the elastic constants and atomic volumes of solute and solvent, given in detail in the book by Alonso and March [12], is based on the use of classical elasticity theory [20]. ΔH_{str} is a band-structure contribution that takes into account the enhancement (or lowering) of the structural stability of the host transition metal when a solute is added. This arises from the well known correlation between the observed crystal structure of transition metals and the number of outer (s + d) electrons [11]. Adding a solute changes the average number of outer electrons and this affects the stability of the host crystal structure. On calculating ΔH_{str}, magnetic effects have also been taken into account, in the way proposed by Miedema and co-workers [11]. ΔS_{ss} is the entropy of mixing, taken equal to ΔS_a. The different contributions to ΔG_{ss} of the hcp solid solution are plotted in figure 3. There is a substantial cancellation between the chemical interaction and elastic terms, and the shape of the free energy curve is due to the structural contribution ΔH_{str}.

Near the two ends of the concentration range, for $x < 0.03$ and $x > 0.91$, the hcp solid solution has a lower Gibbs free energy than the amorphous phase. However, ΔG_{ss} is positive at the Gd-rich end. Thus we can establish an *extended glass-forming region*, indicated in the figure as EGFR, corresponding to compositions $0.06 < x < 0.91$. The lower boundary, $x = 0.06$, limits the region where ΔG_a is negative. However, in order to compare with

experiment it is appropriate to calculate the metastable equilibrium between the solid solution and the amorphous alloy. The long-dashed curves represent the common tangents to the amorphous phase (curve a) and the hcp solid solution (or pure metal at the Gd end). Those tangents determine the minimum and maximum concentrations of Co in amorphous alloys in metastable equilibrium with the solid solution (or pure Gd). These concentrations determine a region usually called the complete glass-forming range (CGFR), in this case $0.32 < x < 0.80$. This calculated CGFR is consistent with the experimental observations [4, 6] of a totally amorphous film for $x > 0.25$ up to at least $x = 0.6$.

3. Interfacial effects in a multilayer configuration

The experiments performed by Riveiro and co-workers [4, 5, 8–10] correspond to bilayer and multilayer configurations. These configurations introduce surface effects and this particular aspect can be included in the calculations to make these more closely reflect the experimental situation. We consider an initial multilayer configuration formed by alternating thin layers of the pure Co and Gd metals. In this case the mismatch between the surfaces of two different metals produces a contribution that displaces the free energy of the initial unmixed state from the (horizontal) zero-line of figure 1 upwards, rendering the initial unmixed configuration less stable compared to the case when no interfacial effects are considered. In other words, the thermodynamic driving force for mixing increases due to the interfacial effect. Following the work of Liu *et al* [21] and of Benedictus *et al* [22], we have calculated the interfacial free energy for the Co/Gd multilayered films as

$$\Delta G_{multilayers} = \zeta\, \Delta G_{interface} \tag{6}$$

where ζ gives the fraction of interfacial atoms in the multilayered system and $\Delta G_{interface}$ is the excess free energy of one mole of interfacial atoms. A multilayered system with a number N of Co layers, each one of thickness d_{Co}, and the same number of Gd layers, each one of thickness d_{Gd}, has $2N - 1$ metal–metal interfaces of thickness $\delta = \delta_{\mathrm{Co}} + \delta_{\mathrm{Gd}}$. Here δ_{Co} is the width of the Co side of the interface and δ_{Gd} the width of the corresponding Gd side of the interface. Before reaction takes place, the fraction of interfacial atoms in the multilayered system is

$$\zeta = x_{\mathrm{Co}}\frac{(2N-1)\delta_{\mathrm{Co}}}{Nd_{\mathrm{Co}}} + x_{\mathrm{Gd}}\frac{(2N-1)\delta_{\mathrm{Gd}}}{Nd_{\mathrm{Gd}}}. \tag{7}$$

Here x_{Co} and x_{Gd} are the atomic fractions of Co and Gd atoms, respectively, in the multilayered system; that is,

$$x_{\mathrm{Co}} = \frac{d_{\mathrm{Co}}/V_{\mathrm{Co}}}{d_{\mathrm{Co}}/V_{\mathrm{Co}} + d_{\mathrm{Gd}}/V_{\mathrm{Gd}}} \tag{8}$$

with V_{Co} and V_{Gd} being the molar volumes of the pure metals, given in table 1. Neglecting entropy contributions, the free energy $\Delta G_{interface}$ of an interface between the two solid metals Co and Gd contains only two contributions [11]; one is due to the chemical interaction of Co and Gd at the interface and the other arises from the strain due to the lattice mismatch:

$$\gamma_{\mathrm{Co-Gd}} = \gamma_{chem} + \gamma_{mismatch}. \tag{9}$$

A good estimate of the lattice mismatch energy per unit contact surface is [11]

$$\gamma_{mismatch} = \left(\frac{1}{2}\right)\frac{\gamma_{\mathrm{Co}} + \gamma_{\mathrm{Gd}}}{3} \tag{10}$$

where γ_{Co} and γ_{Gd} are the usual surface energies of the two pure metals, that is, the metal–vacuum interface energies, given in table 1. The factor $1/3$ relates the surface energy γ of a

metal to the energy $\gamma/3$ of a high-angle grain boundary [23]. The contribution in equation (9) is always positive and makes the initial unreacted multilayered system less stable compared to the case when no contact surfaces exist. On the other hand, the chemical term γ_{chem} has the same origin as ΔH_a and ΔH_{chem} in equations (3) and (5), respectively. So its contribution to the interface energy is equal to the chemical interface enthalpy per unit area:

$$\gamma_{chem} = \frac{\Delta H^0(\text{Co in Gd})}{A V_{\text{Co}}^{2/3}} \tag{11}$$

where ΔH^0(Co in Gd) is the enthalpy of solution of one mole of Co diluted in the metal Gd, and A is a constant depending on the shape of the Wigner–Seitz cell of the atoms in the metal, which has a recommended [11] average value $A = 4.5 \times 10^8$. This chemical contribution can be positive or negative, so it enhances or opposes the effect of $\gamma_{mismatch}$. The expressions in equations (10) and (11) are given per unit area of contact surface. To express those energies *per mole of atoms in contact at the interface*, we can write the chemical term as

$$\gamma_{chem}(\text{per mol}) = p\frac{\Delta H^0(\text{Co in Gd}) + \Delta H^0(\text{Gd in Co})}{2}, \tag{12}$$

where the enthalpies of solution ΔH^0 are given in table 1, or with the equivalent expression

$$\gamma_{chem}\ (\text{per mol}) = [p\gamma_{chem}(\text{per unit surface})]A\frac{V_{\text{Co}}^{2/3} + V_{\text{Gd}}^{2/3}}{2} \tag{13}$$

where γ_{chem}(per unit surface) is given by equation (11). Any Co atom in the interface divides its atomic surface area near equally between contacts with other Co surface atoms, bulk Co atoms and the Gd atoms, and p in the last two equations measures that fraction of the atomic surface of a Co (Gd) atom in contact with Gd (Co) atoms [12], that is, $p = 1/3$. In a similar way,

$$\gamma_{mismatch}\ (\text{per mol}) = [p\gamma_{mismatch}(\text{per unit surface})]A\frac{V_{\text{Co}}^{2/3} + V_{\text{Gd}}^{2/3}}{2}. \tag{14}$$

Then,

$$\Delta G_{interface} = p[\gamma_{mismatch}(\text{per unit surface}) + \gamma_{chem}(\text{per unit surface})]A\frac{V_{\text{Co}}^{2/3} + V_{\text{Gd}}^{2/3}}{2}. \tag{15}$$

Taking into account that only a fraction ζ of the total number of atoms in the system forms part of the interfaces, the excess interfacial free energy is obtained from equation (6). A fair estimate [21] for δ is 5 Å and we take this value here for $\delta_{\text{Co}} + \delta_{\text{Gd}}$. In practice, $\delta \ll d$, but evidently the interfacial energy of the multilayered arrangement can be adjusted by changing the thickness d of the layers.

4. Results, comparison with experiment and discussion

To illustrate the interfacial effects, the points numbered 1–8 in figure 1 represent the free energy before reaction for some of the multilayers prepared by Riveiro and co-workers [4], taking into account the contribution from the free energy of the interfaces. For points 1–7, the values of N, d_{Co} and d_{Gd} were taken in such a way as to simulate the samples in the experiments reported in figure 1 of [4]. In all those cases, $N = 20$, $d_{\text{Gd}} = 50$ Å and the Co layers have increasing thickness: $d_{\text{Co}} = 14$, 28, 56, 70, 105, 140 and 210 Å for points 1–7, respectively. The corresponding Co concentrations in the multilayered system, that can be read from the figure, are obtained from equation (8). Progressing from point 1 to point 7, the fraction ζ of atoms present at the interfaces decreases by an order of magnitude and the interfacial energy

decreases. Point 8 represents different conditions: $N = 20$, $d_{Co} = 122$ Å and $d_{Gd} = 145$ Å. The picture obtained is simple: interfacial effects raise the free energy of the initial multilayered arrangement and the driving force for amorphization is larger. Although the increase of the free energy in the unmixed initial state is modest, because the fraction of interfacial atoms is small due to the relatively large thickness of the individual Co and Gd layers, this effect is locally strong in the neighbourhood of the interfaces, where it triggers the amorphization process, aided by the rapid diffusivity of Co in Gd (the ratio of the diffusion coefficients D(Co in Gd)/D(Gd in Co) is estimated [5] to be around 10).

A fraction of unreacted crystalline Co was observed in the experiments for initial configurations corresponding to points 5–8 in the figure; in those cases d_{Co} is thicker than 100 Å. Even if enough time to complete the reaction is allowed for, only a fraction of the total amount of Co may be consumed when the overall composition of the unreacted multilayer does not fit into the CGFR. This is the case for the compositions corresponding to points 5–7. Those compositions lie outside the CGFR, and this means that amorphous alloys with those compositions do not form if equilibrium is established between the metastable amorphous alloy and the hcp Co-rich solid solution. The case of point 8 is different. The overall composition of the initial multilayer fits into the CGFR and the observation of an unreacted portion may be due to insufficient reaction time. That is, when the individual layers are thick, diffusion kinetics implies that only a fraction of each metal layer may react in the timescale of a given experiment—those parts near the interfaces—while the central part of the layer may remain as an unreacted, thinner pure metal layer. Another set of points, plotted in figure 1 as empty circles and labelled a, b, c, d, e, f, g, h, give the free energies for the initial as-deposited pure Co/Gd multilayers in the recent experiments of [8]. In these multilayers the thickness of the Gd layers is 50 Å and the thickness t of the Co layers varies: $t = 4, 7, 10, 12, 24, 35, 50$ and 100 Å, respectively, for points from left to right. Amorphization at the interfaces occurred in all cases. Residual Gd crystallites appear for t below 50 Å. This result is easy to understand for $t = 4$ and 7 Å (points a and b), because in the free energy diagram of figure 1 the corresponding concentrations lie in a region outside the CGFR. But the observation of unreacted Gd in cases like $t = 10$ and 12 Å (points c and d) is at first surprising because the overall concentrations lie on the CGFR. We defer the interpretation of this result to the last paragraph of this section. Residual Co crystallites were observed for t larger than 35 Å, that is, for points g and h. Again, for point h this can be explained by the fact that the corresponding concentration ($x = 0.86$) does not fit into the CGFR.

Finally we turn to discussing those experiments where the knowledge of the composition of the alloy formed in the reaction was a main objective. The determination of the composition depth profile of the Co/Gd multilayered samples after reaction was performed in [4] and [5] by combining Auger analysis and controlled ion etching. The conclusion was that the structure of the reacted multilayered samples was formed of amorphous regions of composition $Gd_{1-x}Co_x$ with $x = 0.29$–0.35, separated by thin regions of unreacted crystalline Co. Those compositions appeared to have some explanation because the equilibrium phase diagram of the Gd–Co alloy shows a deep eutectic centred at $x = 0.37$ (the eutectic temperature is $T_e = 918$ K) and those compositions are close to the eutectic. The presence of a deep eutectic is a standard criterion for predicting glass formation in alloys, since the stability of the liquid alloy is enhanced for compositions near the eutectic [24, 25]. However, one should keep in mind that the determination of the concentration of the amorphous alloy by the techniques used in [4] and [5] is subject to errors arising from selective re-sputtering and other factors, one of the most important being that the starting multilayers before reaction have rough interfaces due to the intrinsic limitations of the experimental deposition apparatus used in that work, as pointed out above in the introduction. Low-angle reflectivity scans performed recently for the same old samples showed that these were actually alloys with modulated concentrations [8]. For

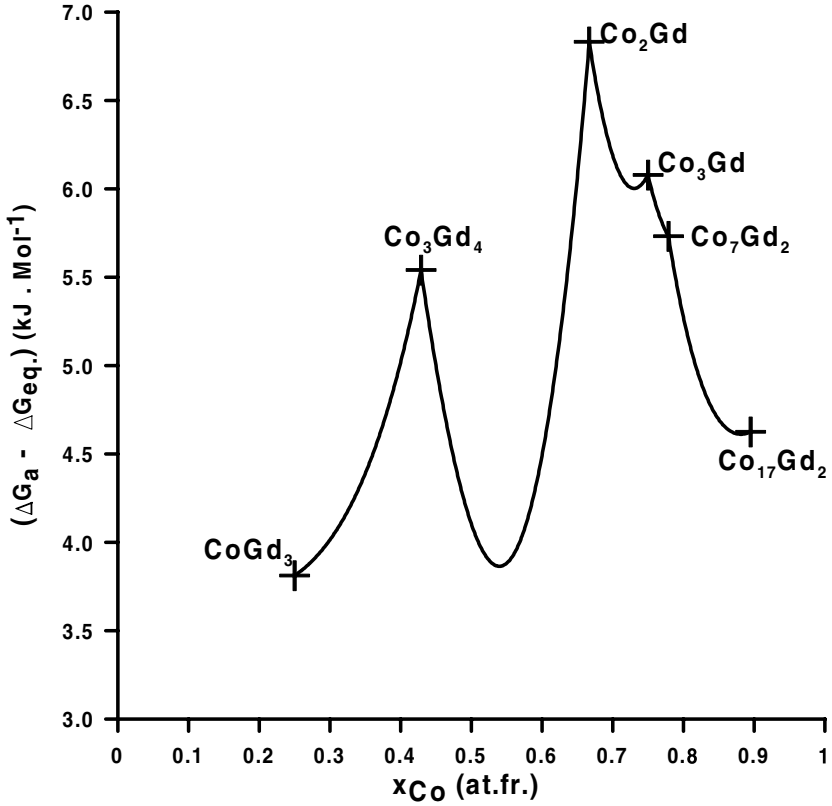

Figure 4. The difference in room temperature free energy between the amorphous $Gd_{1-x}Co_x$ alloys and the equilibrium crystalline phases as a function of Co concentration (see the text). Crosses correspond to concentrations of intermetallic compounds.

this reason, new experiments have been performed [8]. The improvements in the experimental set-up allowed the authors this time to obtain sharp interfaces. In addition, the technique employed to determine the alloy composition profile in the new experiments is more accurate. Another crucial point is that the initial multilayered arrangement was carefully designed so as to promote the evolution of the amorphous alloy towards its preferred composition. For this purpose one of the multilayer configurations studied was composed of amorphous alloy layers with the eutectic $Gd_{0.63}Co_{0.37}$ composition (50 Å thick) alternated with pure crystalline Co layers (of thickness ranging from a few Å to 100 Å). If the eutectic composition were the preferred one, diffusion of Co into the a-$Gd_{0.63}Co_{0.37}$ layers leading to Co enrichment, and to departure from the eutectic composition, should not be expected. In contrast, the experiments [8, 9] give evidence of continuous reaction with a substantial uptake of Co until an alloy with composition near $x = 0.60$ is formed. Experiments were also performed for multilayer configurations formed by alternate layers of a-$Gd_{0.40}Co_{0.60}$ and pure Co, with the striking result that the layers do not react. The interpretation of these experiments is that the preferred composition of the amorphous alloy is not far from $Gd_{0.40}Co_{0.60}$. The measurements of the T-MOKE effect [10] confirm these conclusions and give $Gd_{0.46}Co_{0.54}$ as the preferred one.

We now analyse these results within the framework of the model presented in sections 2 and 3. Let us note in figure 1 that the minimum of the ΔG_a curve occurs at the Co concentration $x = 0.58$. This is the concentration for which the amorphous alloy is most stable with respect

to the unmixed crystalline metals. On the other hand, the crosses in the lower part of the same figure give the calculated free energies of formation of the crystalline ordered compounds present in the equilibrium phase diagram of this alloy [7]. In figure 4 we have plotted a function giving the difference $\Delta G_{cryst}(x) = \Delta G_a(x) - \Delta G_{eq}(x)$. The quantity $\Delta G_a(x)$ is the free energy of the amorphous alloy $Gd_{1-x}Co_x$, given by the curve labelled a in figure 1, and $\Delta G_{eq}(x)$ represents the free energy of the equilibrium crystalline solid for concentration x. At those specific concentrations for which a stable intermetallic compound exists, $\Delta G_{eq}(x)$ is the free energy of that compound (the crosses in figure 1), obtained from equations (3) and (4) with $\eta = 8$. For concentrations in between those of two adjacent compounds, the equilibrium crystalline phase is simply a mechanical mixture of crystallites of those two compounds and $\Delta G_{eq}(x)$ is obtained by the common tangent construction [26] (in our case, just a linear average of the free energies of the two compounds). The curve plotted in figure 4 is then easily calculated from the data in figure 1. The function $\Delta G_{cryst}(x)$ can be interpreted as the free energy change during the crystallization of the amorphous $Gd_{1-x}Co_x$ alloy into a mixture of the two equilibrium compounds. This function presents a sharp minimum centred at $x = 0.54$. That composition is midway between those of two compounds. In the close vicinity of that concentration the driving force for crystallization of the amorphous alloy is smaller that for other concentrations, and the relative stability of the amorphous alloy is higher. Thus, although all concentrations enclosed in the CGFR field may be obtained as amorphous alloys in solid-state reaction experiments, compositions near $x = 0.54$ are expected to be favoured. This prediction is in good agreement with the amorphous composition determined in the recent multilayer experiments by González *et al* [8–10].

The picture emerging is that as a consequence of the fast diffusion of Co in Gd, a kinetic effect whose origin is the tendency for mixing and the small atomic size of Co as compared to Gd, the concentration of Co in the Gd layers increases and, provided that enough Co is available, the mixture can become trapped in a metastable amorphous state preferentially at those concentrations where the following two conditions are met:

(a) the thermodynamic driving force for crystallization is minimal; and
(b) stable crystalline compounds are absent at that concentration.

The second condition is also related to kinetics, since crystallization of the amorphous alloy would require phase separation into two ordered compounds of different compositions. Figure 4 shows that the two conditions are satisfied for compositions near $x = 0.54$.

To close the discussion we return to the recent experiments of González *et al* [8] for pure Co/Gd multilayers. Let us focus on the case for $t = 10$ Å (point c in figure 1). The fact that some Gd remains unreacted indicates that the composition of the amorphous alloy that forms is richer in Co than the nominal composition ($x = 0.37$) in the initial multilayer arrangement. This reinforces the conclusion obtained above from the experiments for a-($Gd_{0.63}Co_{0.37}$)/Co multilayers, that is, the preferred amorphous composition in the Co–Gd alloy is richer in Co than the eutectic composition. One cannot be more quantitative because the thickness of the unreacted Gd layer and the composition of the amorphous alloy formed were not determined. The same lack of detailed information about the fraction of unreacted Gd and Co precludes the analysis of points d–g in figure 1, although it is reasonable to expect that the tendency for a preferred composition of the amorphous alloy may be operating also.

5. Summary

A semiempirical model has been used to successfully explain the wide composition range over which amorphous alloys form in solid-state reaction experiments for Gd–Co bilayers.

The results of experiments with multilayer configurations [4, 5, 8–10] have been analysed with the same model, taking into account the effect of the interfacial energy in promoting the amorphization reaction. The model favours the formation of amorphous alloys with concentration $Gd_{0.46}Co_{0.54}$, a prediction in good agreement with the concentrations found in recent experiments [8–10].

Acknowledgments

This work was supported by DGESIC (Grant PB98-0345) y Junta de Castilla y León (Grant CO01-102).

References

[1] Chaudhary P, Cuomo J J and Gambino R J 1973 *Appl. Phys. Lett.* **22** 337
[2] Camley R E and Stamps R L 1993 *J. Phys.: Condens. Matter* **5** 3727
[3] Hufnagel T C, Brennan S, Payne A P and Clemens B M 1992 *J. Mater. Res.* **7** 1976
Bertero G A, Hufnagel T C, Clemens B M and Sinclair R 1993 *J. Mater. Res.* **8** 771
[4] Colino J, Andrés J P, Riveiro J M, Martínez J L, Prieto C and Sacedón J L 1999 *Phys. Rev.* B **60** 6678
[5] Andrés J P, Sacedón J L, Colino J and Riveiro J M 2000 *J. Appl. Phys.* **87** 2483
[6] Gschneidner K A Jr and Eyring L (ed) 1984 *Handbook of the Chemistry and Physics of Rare Earths* vol 7 (Amsterdam: North-Holland)
[7] Okamoto H 1992 *J. Phase Equilib.* **13** 673
[8] González J A, Andrés J P, Arranz M A, López de la Torre M A and Riveiro J M 2002 *J. Appl. Phys.* **92** 914
[9] González J A, Andrés J P, Arranz M A, López de la Torre M A and Riveiro J M 2002 *J. Phys.: Condens. Matter* **14** 5061
[10] González J A, Andrés J P, López de la Torre M A and Riveiro J M 2002 *J. Magn. Magn. Mater.* **244–245** P1, 547
[11] De Boer F R, Boom R, Mattens W C, Miedema A R and Niessen A K 1988 *Cohesion in Metals* (Amsterdam: North-Holland)
[12] Alonso J A and March N H 1989 *Electrons in Metals and Alloys* (London: Academic)
[13] López J M, Alonso J A and Gallego L J 1987 *Phys. Rev.* B **36** 3716
[14] Rodríguez C, de Tendler R H, Gallego L J and Alonso J A 1995 *J. Mater. Sci.* **30** 196
[15] Johnson W L 1992 *Materials Interfaces* ed D Wolf and S Yip (London: Chapman and Hall) p 516
[16] Weber A W and Bakker H 1988 *Physica* B **153** 93
[17] Van der Kolk G, Miedema A R and Niessen A K 1988 *J. Less-Common Met.* **145** 1
Loeff P I, Weber A W and Miedema A R 1988 *J. Less-Common Met.* **140** 299
[18] Flory P J 1942 *J. Chem. Phys.* **10** 51
[19] Weber A W 1987 *J. Phys. F: Met. Phys.* **17** 809
[20] Eshelby D 1956 *Solid State Phys.* **3** 79
[21] Liu B X and Zhang Z J 1996 *J. Phys.: Condens. Matter* **8** L165
[22] Benedictus R, Böttger A and Mittemeijer E J 1996 *Phys. Rev.* B **54** 9109
[23] Miedema A R and den Broeder F J 1979 *Z. Metall.* **70** 14
[24] Massalski B, Kim Y W, Vassamillet L F and Hooper R W 1981 *Mater. Sci. Eng.* **47** 1
[25] Walser R M and Bené R W 1976 *Appl. Phys. Lett.* **28** 624
[26] Hillert M 1998 *Phase Equilibria, Phase Diagrams and Phase Transformations: their Thermodynamic Basis* (Cambridge: Cambridge University Press)